Infection, Genetics and Evolution 73 (2019) 390–400

Contents lists available at ScienceDirect

Infection, Genetics and Evolution

journal homepage: www.elsevier.com/locate/meegid

Research paper

Immunoinformatics and structural vaccinology driven prediction of multi-epitope vaccine against Mayaro virus and validation through *in-silico* expression

Shahzeb Khan[a,1], Abbas Khan[b,1], Ashfaq Ur Rehman[b], Irfan Ahmad[a], Saif Ullah[a], Abdul Aziz Khan[c], Syed Shujait Ali[a], Sahib Gul Afridi[d], Dong-Qing Wei[b,*]

[a] Centre for Biotechnology and Microbiology, University of Swat, Swat, Khyber Pakhtunkhwa, Pakistan
[b] Department of Bioinformatics and Biological Statistics, School of Life Sciences and Biotechnology, Shanghai Jiao Tong University, Shanghai 200240, PR China
[c] Laboratory of Animal and Human Physiology, Department of Animal Sciences, Quiad-i-Azam University, 45320 Islamabad, Pakistan
[d] Department of Biochemistry, Abdul Wali Khan University Mardan, Pakistan

ARTICLE INFO

Keywords:
Mayaro virus
Vaccine
B-cell
T-cell
Epitopes
Docking
In silico cloning

ABSTRACT

The *Mayaro* virus (MAYV) belongs to genus "*Alphavirus*" and family "Togaviridae". *MAYV* has distribution in the Amazonia, Central and Northeastern regions of Brazil. The abundance of mosquito vector *Haemagogus janthinomys* has major role in the outbreaks of arthralgia disease in Brazil. Vaccination or immunization is an alternative approach for the protection against this disease. To search the effective candidate for vaccine against *Mayaro virus*, various immunoinformatics tools were used to predict both the B and T cell epitopes from five structural polyproteins (capsid, E2, 6K, E3and E1). A multi subunit vaccine was designed and the final sequence was modeled for docking with TLR-3. Human b defensin based on previous studies was used as linker. The docked complexes of vaccine-TLR-3 were then subjected to dynamics stability and RMSD and RMSF results suggested that the complexes are stable. Further, to validate our final vaccine construct, in silico cloning was carried out using *E. coli* as host. The CAI value of 0.96 suggests that the vaccine construct properly expresses in the host. The current findings will be useful for the future experimental validations to ratify the immunogenicity and safety of the supposed structure of vaccine, and ultimately to treat the *Mayaro virus*, associated infections.

1. Introduction

The *Mayaro* virus (MAYV) belongs to the genus "*Alphavirus*" and family "Togaviridae". MAYV has distribution in the Amazonia, Central and Northeastern regions (Coimbra et al., 2007; Figueiredo, 2007) of Brazil. The abundance of mosquito vector *Haemagogus janthinomys* has a significant role in the outbreaks of arthralgia disease in these areas(da Rosa et al., 1998). This virus remains endemic in the Amazon region of Brazil and has high sero-positivity levels within populations (typically 5–60%)(Anderson et al., 1957; Pinheiro et al., 1981). *Aedes aegypti* abundance in urban Brazil is a major reason of distribution of the MAYV in urban centers of Brazil (Long et al., 2011; Rosa et al., 2000). The short life (around 3 days) of this virus is a major hindrance in the isolation of virus from serum samples. However, migratory birds and primates are considered to play an important role in enzootic virus circulation (Vasconcelos et al., 1998).

Like other *Alpha viruses*, *Mayaro virus* also an enveloped virus with a 70 nm (diameter) icosahedral capsid. Its single-stranded RNA genome (without the 5′ cap and 3′ poly (A) nucleotides) contained 11,429 nucleotides (Lavergne et al., 2006; Mourão et al., 2012). The genome of the MAYV comprises of total two open reading frames (ORFs), 5′ untranslated region (UTR) basically encodes for four non-structural proteins (nsP1-nsP4), and the 3′ non-coding region (NCR)encodes for structural proteins viz., C (Capsid protein (C)), E3 (spike glycoprotein E3), p62, E2 (spike glycoprotein E2), E1 (spike glycoprotein E1), and 6K (Lavergne et al., 2006). Among the non-structural proteins (nsP) the nsP1 involves in capping, nsP2 express protease activity and the nsP4 has the polymerase activity. Interestingly the lipid part of the envelope is concerned with the stability and infectivity of the virus particle in host cells (Sousa et al., 2011). After the entrance into the host cell, the viral genomic RNA released into the cell cytoplasm, and two ORFs translations into proteins are initiated. Based on sequences analysis,

* Corresponding author.
E-mail addresses: abbaskhan@sjtu.edu.cn (A. Khan), azizkhan@sjtu.edu.cn (A.A. Khan), shujaitswati@uswat.edu.pk (S.S. Ali), dqwei@sjtu.edu.cn (D.-Q. Wei).
[1] Contributed equally.

https://doi.org/10.1016/j.meegid.2019.06.006
Received 26 March 2019; Received in revised form 22 May 2019; Accepted 3 June 2019
Available online 04 June 2019

two genotypes D and L are identified in MAYV, whereas genotype D has distribution in Bolivia, Brazil, French Guyana, Peru, Surinam and, Trinidad, the distribution of genotype L is confined to Brazil's North Central Region (Powers et al., 2006).

The scientific community relies on immunoinformatics approaches to develop a fast, reliable and effective vaccine to control pathogenic diseases. The antigenic nature of pathogen's secretory proteins makes them an ideal candidate for vaccine development to predict B and the T cell epitopes (Khatoon et al., 2017). During infection after the activation of antigen-displaying cells, the T cells act as effectors to kill all infected cells. Peptide fragments of the pathogen bind with MHC molecules, which appear on infected host cell surfaces. The MHC molecule is certainly capable of binding with Peptides firmly as pathogens attempt to cause mutation in the MHC molecule epitope.

Consequently, the MHC molecule has a great binding affinity with a diverse range of peptides (Suhrbier et al., 2012). Vaccination works by stimulating the host body's immune system, the natural fighting mechanism that is activated in a diseased condition (Khan et al., 2018). The MHC molecules play an important role by presenting antigen on the surface to improve immune system can be useful in vaccinations and immune-therapies (Khatoon et al., 2017) which is considered a safe, fast and effective method to curtail and control the vector-borne parasitic diseases. Initially, the fast development of immunization was made to counter infection, involves the inoculation of autoclaved or live pathogens. Howeve, due to safety concern, such practices are abandoned for human use. The current technological advancement, new sequencing methodologies, better understanding of pathogens and human's immune system revolutionized the field of immunology and are considered very important in vaccine development (Ali et al., 2019). Immunoinformatics approaches are advance and fast techniques to develop effective and thermodynamically stable multi-epitope subunit vaccine. Therefore, we designed a multi-epitope subunit model vaccine, which can activate both the humoral and cell-mediated based immune responses in a pathogenic condition. The ultimate vaccine construct was then docked against TLR-3, and molecular dynamics simulation was carried out to test the stability. In silico expression was carried out in *E. coli* host for the expression and further vaccine validation. Current findings will aid the development of vaccine candidates against Mayaro virus' infections.

2. Methodology

2.1. Collection of MAYV structural polyprotein

The complete amino acid sequences of structural polyprotein of MAYV (ALJ56197.1) were retrieved from Gene Bank Database, NCBI (https://www.ncbi.nlm.nih.gov/) in standard FASTA format (Accession number: ALJ56197.1) (Benson et al., 2008). The overall flow of the work is presented in Fig. 1.

2.2. CTL (cytotoxic T lymphocytes) epitope prediction

The prediction of CTL epitopes (for the structural polyprotein of MAYV) was performed with the help of an online web tool NetCTL 1.2 (http://www.cbs.dtu.dk/services/NetCTL/) (Larsen et al., 2007). The epitopes prediction focused on three key components, i.e., MHC-I binding peptide prediction, proteasomal C-terminal cleavage, and the transportation efficiency Transporter Associated with Antigen Processing (TAP). The artificial neural networks used to estimate the MHC-I binding and proteasomal C-terminal cleavage, whereas weight matrix was used to calculate the efficacy of TAP transporter. The threshold set for the prediction of CTL epitopes was 0.75.

2.3. HTL (helper T-cell) epitope prediction

Five total epitopes of 15-mer length for human alleles (HLA-DRB1*01:01, HLA-DRB1*01:02, HLA-DRB1*01:03, HLA-DRB1*01:04, HLA-DRB1*01:05) were predicted for a structural polyprotein of MAYV utilizing online server IEDB (http://www.iedb.org/)(Vita et al., 2014). The peptide affinity for each receptor is based on IC50 score given to each epitope. Peptides having higher binding affinity must have an IC50 value < 50 nM, whereas the IC50 score < 500 nM and < 5000 nM point to an intermediate and low binding affinity of predicted epitopes respectively. The score of the percentile rank is inversely linked to the binding affinity of the epitop, which means that the lower the percentile rank the higher the binding affinity. In order to prove our work that the predicted HTL epitopes will have the ability to activate Th1 type immune response followed by the IFN-γ production, the predicted HTL epitopes were subjected to the IFNepitope server (http://crdd.osdd.net/raghava/ifnepitope/index.php) (Dhanda et al., 2013) using predict option. Motif and SVM hybrid was selected as the approach and IFN-gamma versus other cytokine as a model of prediction. IFNs mostly has a protective role against infectious diseases and minimize host damage. IFNs are used in chemotherapy of cancer (Green et al., 2016; Hiramatsu et al., 2015), enteroviral myocarditis treatment (Kühl et al., 2012), and hepatitis treatments (Lin et al., 2016). It is used as adjuvants in combination with antigen in vaccine designing against multiple diseases (Toporovski et al., 2010) like HPV (Öhlschläger et al., 2009), HIV (Abaitua et al., 2006), (Jiang et al., 2007) and influenza (James et al., 2007).

2.4. Toxicity prediction

To ensure the non-toxic nature of the selected epitopes an online tool ToxinPred was used for prediction of epitopes toxicity the server predicts the toxicity of epitopes based on the physiochemical properties (http://crdd.osdd.net/raghava/toxinpred/) (Gupta et al., 2013).

2.5. B cell epitope prediction

B cell epitopes are identified and bound by the receptors associated with the B- lymphocytes on its surface are characterized as antigenic factors. B-cell epitopes play a much larger role in the host antibody production plan. An online web tool BCPred (http://ailab.ist.psu.edu/bcpred/) (EL-Manzalawy et al., 2008) is a new technique that employs kernel method for prediction of linear B cell epitopes. Kernel methods consist of different algorithms used for pattern analysis, a well-known member of this group is SVM (support vector machine). The prediction and output performance of BCPred (AUC = 0.758) is based on the SVM along with the employment of AAP (Amino acid pair antigenicity) (AUC = 0.7) (EL-Manzalawy et al., 2008). The AAP is used for prediction of linear B cell epitopes.

Furthermore, ElliPro an online server (http://tools.iedb.org/ellipro/) (Ponomarenko et al., 2008) was utilized for prediction conformational B-cell epitopes. The ElliPro results are based on Thornton's technique and residue clustering algorithm, the Modeller program is used for antibody epitope prediction in an input structure, whereas Jmol viewer is employed for the visualization of the epitopes. ElliPro assigns PI (protrusion index) score to each predicted epitope., Using several ellipsoids the 3D shape of the epitope is defined and for each residue, the PI value is accurately described based on the centre of mass of each residue, which is located in the outer region of the largest promising ellipsoid. A Residue with larger value has better solvent accessibility.

2.6. Construction of multi-epitope vaccine sequence

A vaccine sequence was carefully constructed using the CTL and HTL epitopes predicted by the above-employed immunoinformatics approaches. These CTL and HTL epitopes were joined with the help of AAY and GPGPG (Sabourin et al., 2007) used as linkers, and adjuvant was added (Lee et al., 2014) respectively.

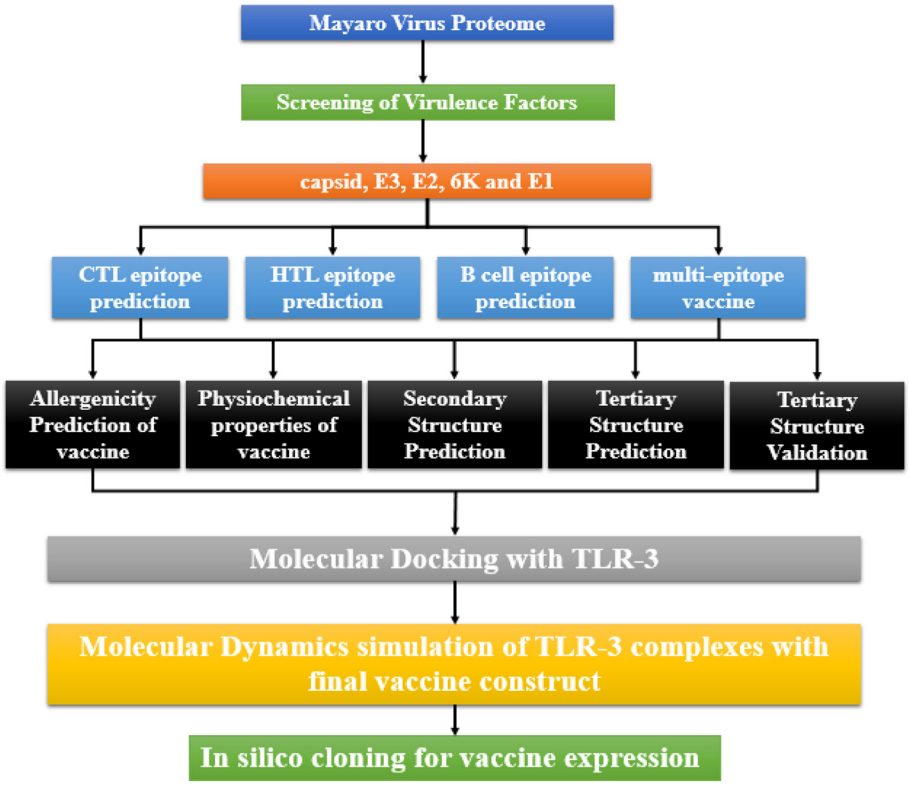

Fig. 1. The figure represents the overall flow of the work. The methodology was divided into five parts: data retrieval, epitopes prediction, epitopes modelling, molecular docking and simulation and validation through in silico expression.

2.7. Allergenicity prediction of the vaccine

A group of varied algorithms were used to predict the allergenic score for the constructed vaccine sequence with great accuracy. AlgPred an online web server (http://www.imtech.res.in/raghava/algpred/) (Saha and Raghava, 2006) was used for allergenicity prediction. The accuracy acquired for this approach is about 85% at a 0.4 threshold. The server employs six different approaches for the prediction of allergenicity with incredible accuracy.

2.8. Antigenicity prediction of the vaccine

The antigenicity prediction of the constructed vaccine sequence was performed on VaxiJen server with high accuracy at 0.4 thresholds for bacteria selected as a model organism. The server is based solely on the physiochemical properties for prediction of antigenicity for a given amino acid sequence. (http://www.ddg-pharmfac.net/vaxijen/VaxiJen/VaxiJen.html).

2.9. Physiochemical properties and domain identification

The physiochemical properties such as amino acid composition of the vaccine, theoretical pI, molecular weight, instability index, in vitro and in vivo half-life, aliphatic index and grand average of hydropathicity (GRAVY) were calculated for the final vaccine construct utilizing an online web tool the ProtParam (http://web.expasy.org/protparam/) (Gasteiger et al., 2005).

2.10. Secondary structure prediction

PSIPRED (McGuffin et al., 2000) is a freely available web tool (http://bioinf.cs.ucl.ac.uk/psipred/) for protein secondary structure prediction for the given amino acid sequences with high accuracy. The server was employed for the prediction of the secondary structure for the final multi-epitope subunit vaccine.

2.11. Tertiary structure prediction

RaptorX (http://raptorx.uchicago.edu/) an online freely available server was used to predict 3D structure for the vaccine sequence (Källberg et al., 2012). RaptorX also predicts secondary structure, contacts, solvent accessibility, disordered regions and binding sites for the input sequence. The server allocates confidence scores to point out the excellence of the predicted 3D structure: The *P*-value is assigned for the comparative global quality of the model, whereas GDT (global distance test) and uGDT (un-normalized GDT) values assigned for the model's absolute global quality. The modelling error for each residue is identified with RaptorX. For visualization of the predicted 3D model, Pymol software was used.

2.12. Refinement of the tertiary structure

The 3D structure for the predicted multi-epitope subunit vaccine was refined using an online web tool Galaxy Refine (http://galaxy.seoklab.org/) (Ko et al., 2012). The server employs CASP10 refinement method for protein's side chain reconstruction, repacking as well as MD simulations for relaxation of the 3D structure. Galaxy refine one of the best available server (Based on the CASP10) for the overall improvement of both the global and the local quality of the given structure generated by utilizing the best protein structure prediction web tools available.

2.13. Tertiary structure validation

The validation of the 3D model of the vaccine construct was performed on ProSA-web, ERRAT and RAMPAGE. ProSA-web (https://prosa.services.came.sbg.ac.at/prosa.php) is a freely available web server frequently used for validation of the input 3D model

(Wiederstein and Sippl, 2007). ProSA assigns a quality score for the input structure if the score lies outside a range typical for native proteins, the structure most likely have errors. A 3D molecule view is included in the ProSA-web results in order to facilitate the detection of the problematic part indicated by the assigned score. Another validation server known as ERRAT (http://services.mbi.ucla.edu/ERRAT/) (Colovos and Yeates, 1993) was used to find out the non-bonded interactions within the structure. RAMPAGE an online web tool (http://mordred.bioc.cam.ac.uk/~rapper/rampage.php) was employed for the analysis of Ramachandran plot, RAMPAGE employs the PROCHECK principle for validation of the protein structure by using Ramachandran plot and plots for Glycine as well as Proline residues.

2.14. Molecular docking of vaccine with the receptor

PatchDock (http://bioinfo3d.cs.tau.ac.il/PatchDock/) server was used for TLR-3 (PDB ID: 1ziw) – vaccine docking (Schneidman-Duhovny et al., 2005), to show the progress of the immune response. PatchDock carries out a calculation for the molecular docking. The calculation by PatchDock involves three basic stages, i.e. atomic shape portrayal; surface fixes coordinating as well as separating and scoring. PatchDock separates the surface of both the input molecules into small patches as per the proper surface shape. Such patches then correlate to complex patterns which can differentiate visually between the puzzle pieces. Only after the identification of all these small patches, their superposition is accomplished by using shape matching algorithms. Moreover, FireDock (Fast Interaction Refinement in Molecular Docking) (Andrusier et al., 2007) web tool (http://bioinfo3d.cs.tau.ac.il/FireDock/) had been used to optimize as well as re-score the rigid body molecular docking solutions. It provides the best ten solutions for final refinement. All of the highly refined models were entirely based on the binding value. This overall score contains Atomic contact energy as well as Van Der Waals interaction, partial electrostatics and estimations of the binding energy.

2.15. Molecular dynamics simulations

AMBER 14 (Pearlman et al., 1995) molecular dynamics package was used to conduct MD simulations for all the selected complexes. Addition of Na + ions and hydrogen helped to neutralize the systems counter with the application of "tLeap" package of Amber. A TIP3P water box of 12.0Å was used. Energy minimization of the complexes was carried out on AMBER 14 using SANDER module at two stages (each of 6000 steps) in order to remove all the constraints atoms in the systems. The minimized complexes were subjected to PMEMD.cuda (Salomon-Ferrer et al., 2013) for the accomplishment of MD simulations. The SHAKE and Particle-Mesh Ewald (PME) method with a non-bond contacts cutoff radius of 10A°, was used for long-term interactions. Constant temperature and pressure with isotropic scaling was applied for equilibration of 10,000 ps time, followed by a total of 30 ns simulation for the final vaccine construct and 50 ns for the vaccine-TLR-3 complex.

For post-simulation trajectories analysis, 2.0 ps time scale was used and for trajectory, sampling using CPPTRAJ and PTRAJ (Roe and Cheatham III, 2013) implemented in AMBER 14. Eqs. (1) and (2) were used to calculate the RMSD and RMSF.

$$\mathrm{RMSD} = \sqrt{\frac{\sum_{i=0}^{N} [m_i * (X_i * Y_i)^2]}{M}} \quad (1)$$

where;N, mi and M = number and masses of atoms and total mass,Xi and Yi = coordinate vector for target and reference atom *i*,If the RMSD is not mass-weighted, all mi = 1 and M = N.

$$\text{Thermal factor or B} - \text{factor} = [(8\pi * * 2)/3]\,(\mathrm{msf}) \quad (2)$$

In silico cloning optimization of vaccine protein.

In order to express the multi-epitope subunit vaccine in a decent vector for expression, reverse translation, as well as optimization of codons, were conducted in the Java Codon Adaptation Tool (JCat). Codon optimization was essential to express the final vaccine structure in host *E. coli* (strain K12) because the codon usage by *E. coli* is different from the native host. Three extra options were considered to evade the rho-independent transcription termination, prokaryote ribosome binding site and restriction enzymes cleavage sites. JCat output consists of codon adaptation index (CAI) and percentage GC content to confirm the high-level of protein expression. However, to clone the adapted final vaccine gene sequence in *E. coli* (pET-28a (+) vector), *Xho*I and *Nde*I restriction sites were added to the N and C-terminal of the nucleotide sequence, respectively. At last, the optimized sequence (with restriction sites) was inserted into the pET-28a (+) vector using SnapGene tool to make sure the vaccine expression.

3. Results

3.1. Proteins sequences retrieval for B and T-cell epitopes prediction

Mayaro virus structural polyproteins (capsid, E3, E2, 6K and E1) amino acid sequence was retrieved from NCBI (https://www.ncbi.nlm.nih.gov/). The amino acid sequence was used to predict the B and T cell epitopes for designing the multi-epitope subunit vaccine.

3.2. Cytotoxic T lymphocytes (CTL) epitopes prediction

Total 32 CTL epitopes of 9-mer lengths were predicted for the structural polyproteins using an online web tool NetCTL1.2 (http://www.cbs.dtu.dk/services/NetCTL/) as shown in Table 1. Based on high binding affinity scores, only seven non-allergenic epitopes were selected as final CTL epitopes.

3.3. Helper T lymphocytes (HTL) epitopes prediction

HTL epitopes for five human alleles HLA-DRB1*01:01, HLA-DRB1*01:02, HLA DRB1*01:03, HLA-DRB1*01:04, HLA-DRB1*01:05 were predicted by MHC-II prediction module of IEDB (http://www.iedb.org/).The positions of selected HTL epitopes were 1218–1232 (HLA-DRB1*01:01), 1219–1233(HLA-DRB1*01:01), 1226–1240 (HLA-DRB1*01:02), 687–701 (HLA-DRB1*01:02), 461–475 (HLA-DRB1*01:02), 1156–1170 (HLA-DRB1*01:03), 791–805 (HLA-DRB1*01:03), 38–52 (HLA-DRB1*01:03), 40–54 (HLA-DRB1*01:04), 762–776 (HLA-DRB1*01:04), 615–629 (HLA-DRB1*01:05), and 616–630 (HLA-DRB1*01:05) as shown in Table 2. The selection of both CTL and HTL epitopes were based purely on their non-allergenic property and high binding affinity scores.

3.4. Toxicity prediction

The non-toxic nature of 7 CTL and 12 HTL epitopes were confirmed with the help of ToxinPred server. The results obtained from ToxinPred are shown in Table 2, and these selected epitopes (7 CTL and 12 HTL) can be safely used.

3.5. Construction of multi-epitope subunit vaccine

The 7 CTL epitopes and 12 HTL selected epitopes based on the binding affinity score were joined with the help of AAY linker for CTL epitopes and GPGPG linker for HTL epitopes to form the final vaccine construct. The structure of the final vaccine construct is given in Fig. 2, while the IFN-epitopes are tabulated in supplementary materials Table S1.

3.6. B cell epitopes prediction for MAYV structural polyprotein

Among Linear B cell epitopes, (Table 3) predicted by an online

Table 1
List of Predicted T-cell epitopes. Final epitopes were selected on the basis of C-terminal cleavage, TAP scores and toxicity.

Residue no	Peptide sequence	MHC Binding affinity	Rescale binding affinity	C-terminal cleavage affinity	Transport affinity	Prediction score	MHC-I Binding	Toxicity
143	NADLARLSY	0.5515	2.3418	0.965	2.699	2.6215	Yes	Non-Toxin
149	LSYKKSSKY	0.3063	1.3007	0.9758	3.288	1.6115	Yes	Non-Toxin
167	AMKSDASKY	0.1212	0.5146	0.974	3.235	0.8225	Yes	
169	KSDASKYTH	0.1746	0.7414	0.6397	0.528	0.811	Yes	
302	NSEGYYDLL	0.1846	0.7837	0.2656	0.935	0.8702	Yes	
325	STANHFNAY	0.7346	3.1191	0.9731	3.105	3.4203	Yes	
362	QADATDGTL	0.1414	0.6003	0.8671	0.853	0.773	Yes	
382	KTDTHDHTK	0.3137	1.3317	0.8098	0.384	1.4724	Yes	
385	THDHTKIRY	0.1135	0.4819	0.9424	2.596	0.753	Yes	
472	GIELPCTTY	0.1276	0.5418	0.9778	2.707	0.8238	Yes	
483	TTAETSEEI	0.1425	0.6051	0.8662	0.557	0.7629	Yes	
487	TSEEIDMHM	0.1628	0.6914	0.6925	0.013	0.7959	Yes	
515	TVNGRTVRY	0.2104	0.8934	0.9788	2.957	1.1881	Yes	
536	TTDKTINSC	0.1847	0.7842	0.0584	0.194	0.7832	Yes	
544	CTVDKCQAY	0.3011	1.2783	0.8967	2.994	1.5625	Yes	
553	VTSHTKWQF	0.2382	1.0113	0.5935	2.519	1.2263	Yes	
702	LLSLAASVY	0.3247	1.3785	0.8654	2.991	1.6578	Yes	Non-Toxin
747	ASFAEGMAY	0.3643	1.5466	0.7428	3.375	1.8268	Yes	Non-Toxin
768	LTGPLALLI	0.1637	0.695	0.3457	0.187	0.7562	Yes	
778	TTCCARSLF	0.1868	0.7933	0.5792	2.549	1.0077	Yes	
809	HTAIIPNQV	0.1809	0.7679	0.8711	0.052	0.9012	Yes	
844	LEPTLNLEY	0.1454	0.6171	0.9519	2.832	0.9015	Yes	
849	NLEYITCDY	0.4488	1.9055	0.9685	2.885	2.195	Yes	
883	KCAVFTGVY	0.1563	0.6637	0.3991	3.017	0.8744	Yes	
945	TVNQTVEAY	0.3077	1.3066	0.7505	2.918	1.565	Yes	
983	IVVYKGEVY	0.1119	0.4752	0.878	3.265	0.7702	Yes	
1012	RTLDSRDLY	0.3347	1.4211	0.7805	3.219	1.6991	Yes	Non-Toxin
1031	AAGNIHVPY	0.1372	0.5824	0.9741	2.813	0.8691	Yes	
1085	SMDIADSAF	0.2567	1.09	0.9419	2.58	1.3602	Yes	
1110	STCTHSSDF	0.2233	0.9482	0.1417	2.622	1.1006	Yes	Non-Toxin
1115	SSDFGGIAV	0.2801	1.189	0.7469	0.209	1.3115	Yes	
1161	STASAAPSF	0.1348	0.5723	0.4537	2.478	0.7642	Yes	Non-Toxin

server BCPREDS, ten epitopes of 20-mer lengths with a score of 0.9 and above were selected for further analysis. Ellipro suit was utilized to predict the conformational B-cell epitopes. Total 44 residues from 1 to 20 and 290–313 with a score of 0.94 and 0.715 respectively (default threshold was 0.5, default maximum distance was 6), were considered as the discontinuous B-cell epitopes (Fig. 3). Moreover, in the first chain of the discontinuous epitope, the start and end residues were asparagines and lysine with residue score of 0.941 and 0.941, respectively. In the second chain, start and end residues were represented by serine and valine having the residue score of 0.47 and 0.35, respectively.

3.7. Prediction of Allergenicity

The AlgPred server was used to check the Allergenicity of vaccine construct. The allergenicity score of constructed multi-epitope vaccine was −1.20 (default threshold set at −0.4) and found to be non-allergenic.

3.8. Antigenicity of the vaccine construct

VaxiJen server predicted the antigenic nature of our final multi-epitope subunit vaccine. The score predicted was 0.8, while 0.4 was used as a threshold for this analysis. The results suggest that our vaccine candidate possess strong antigenic properties that will help to provoke the immune response. The scores obtained for each vaccine from the server are given in the supplementary material (Table S2).

3.9. Prediction physiochemical parameter

ProtParam server was employed to calculate the nine physiochemical properties of the final vaccine construct. The molecular weight of 31.7 kDa and theoretical protrusion index (PI) of 8.54 of the vaccine is indicating the basic nature of the vaccine. The estimated in vivo half-life in *E. coli* was > 10 h. The stability of the vaccine in the test tube was determined by the instability index, and this value for the final vaccine

Table 2
Helper T-Cell epitopes for selected proteins of *Mayaro virus* using IEDB MHC-II module.

S. no	Allele	Start	End	Peptide sequence	Method	Percentile rank	Toxicity
1	HLA-DRB1*01:01	1218	1232	AGGVGLLIALAVLIL	Consensus (comb.lib./smm/nn)	0.28	Non-Toxin
2	HLA-DRB1*01:01	1219	1233	GGVGLLIALAVLILV	Consensus (comb.lib./smm/nn)	0.28	Non-Toxin
3	HLA-DRB1*01:02	1226	1240	ALAVLILVIVTCVTL	sturniolo	0.01	Non-Toxin
4	HLA-DRB1*01:02	687	701	PTITIVVVIAVSVVV	sturniolo	0.02	Non-Toxin
5	HLA-DRB1*01:02	461	475	GRERFTVRPHHGIEL	sturniolo	0.37	Non-Toxin
6	HLA-DRB1*01:03	1156	1170	SVIHFSTASAAPSFV	NetMHCIIpan	0.2	Non-Toxin
7	HLA-DRB1*01:03	791	805	GSFLVAMSIGSAVAS	NetMHCIIpan	0.27	Non-Toxin
8	HLA-DRB1*01:03	38	52	RQMQQLIAAVSTLAL	NetMHCIIpan	0.54	Non-Toxin
9	HLA-DRB1*01:04	40	54	MQQLIAAVSTLALRQ	NetMHCIIpan	0.7	Non-Toxin
10	HLA-DRB1*01:04	762	776	SMFWMELTGPLALLI	NetMHCIIpan	0.74	Non-Toxin
11	HLA-DRB1*01:05	615	629	PTLLSYRTLGAEPVF	NetMHCIIpan	0.65	Non-Toxin
12	HLA-DRB1*01:05	616	630	TLLSYRTLGAEPVFD	NetMHCIIpan	0.73	Non-Toxin

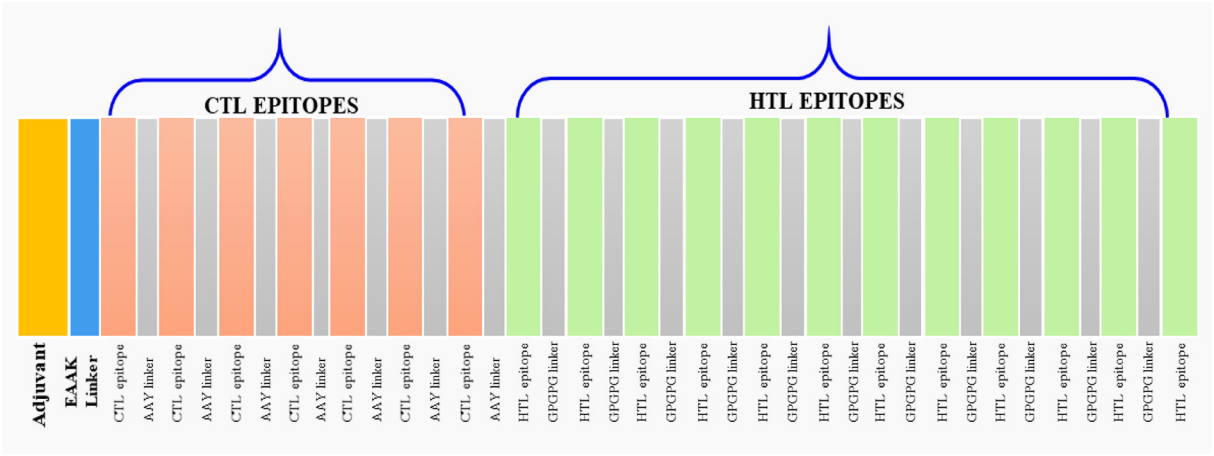

Fig. 2. Structure of the final multi-epitope vaccine construct. CTL and HTL epitopes along with linkers are depicted.

Table 3
Table of Linear B-cell epitopes predicted by BCPred server.

S. no	Position	Epitope	Score
1	73	STCTHSSDFGPGPGAGGVGL	1
2	159	VVVGPGPGGRERFTVRPHHG	1
3	235	STLALRQGPGPGRQMQQLIA	1
4	96	LAVLILGPGPGGGVGLLIAL	1
5	190	HFSTASAAPSFVGPGPGGSF	1
6	258	TLALGPGPGPTLLSYRTLGA	1
7	133	LVIVTCVTLGPGPGPTITIV	1
8	295	GAEPVFDGPGPGSMFWMELT	1
9	213	MSIGSAVASGPGPGMQQLIA	0.999
10	13	LSYKKSSKYAAYSTASAAPS	0.913

construct was 26.66 (the value below 40 is considered as stable in nature). The aliphatic index value was 104.33, which indicates the thermostable nature at variable temperature. The Grand Average of Hydropathy value of the vaccine was 0.614, suggesting its hydrophilic nature.

3.10. Secondary structure prediction

PSIPRED server utilized to predict secondary structure for the final vaccine construct. The results obtained from the server showing the presence of Alpha helix (Hh): 28.04%, Extended strand (Ee): 29.91%, Beta-turn (Tt): 2.18%, Random coil (Cc): 39.88% in the vaccine structure. Graphical representation of the depicted structure is given in Fig. 4.

3.11. Homology modelling and tertiary structure refinement

The 3D structure for the final multi-epitope subunit vaccine, Fig. 5(A), was generated with the RaptorX server and the output model was partitioned into two domains. Multi-template based approach was used for homology model, however for “domain1” templates with PDB ID: 6ENO, 3TSY, 6H02, 4ADY, 4WKY and for “domain 2” templates with PDB ID: 5ZQ6, 3J0C, 3MUW, 3DM0, 3OEP were considered. The finest template for protein model was (PDB ID: 6ENO-A) with its *P*-value of 6.71 − e the score obtained for the template was 65 having 24% sequence identity while the remaining templates were found to be less identical. Galaxy Refine server carried out the structural refinement. Out of the provided 5 models by the server, model 1 was selected to be the finest one, the decision was based on several parameters comprising GDT-HA (0.9307), RMSD (0.468), MolProbity (2.812), Clash score (38.6), Poor rotamers (1.8) and Ramachandran plot (89.7). Model 1 was finalized for further analysis. The superimposed structure of the template and vaccine construct along with the templates scores is given in supplementary materials (Fig. S1).

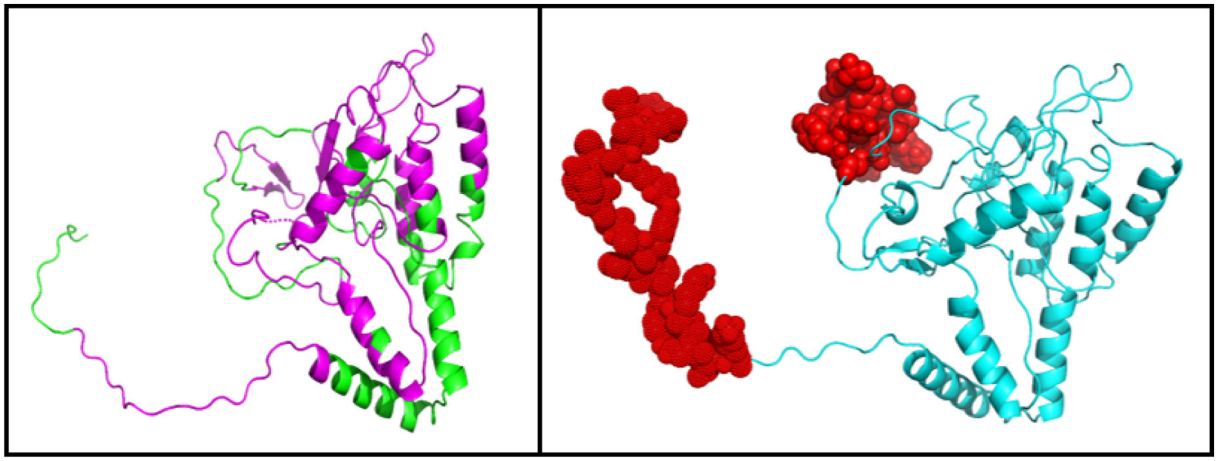

Fig. 3. Prediction of B-cell epitopes for the construct of the final subunit vaccine. (A) The conformational B-cell epitopes are portrayed as red spheres in in in the final vaccine structure (B) linear B-cell epitopes shown in magenta colour. (For interpretation of the references to colour in this figure legend, the reader is referred to the web version of this article.)

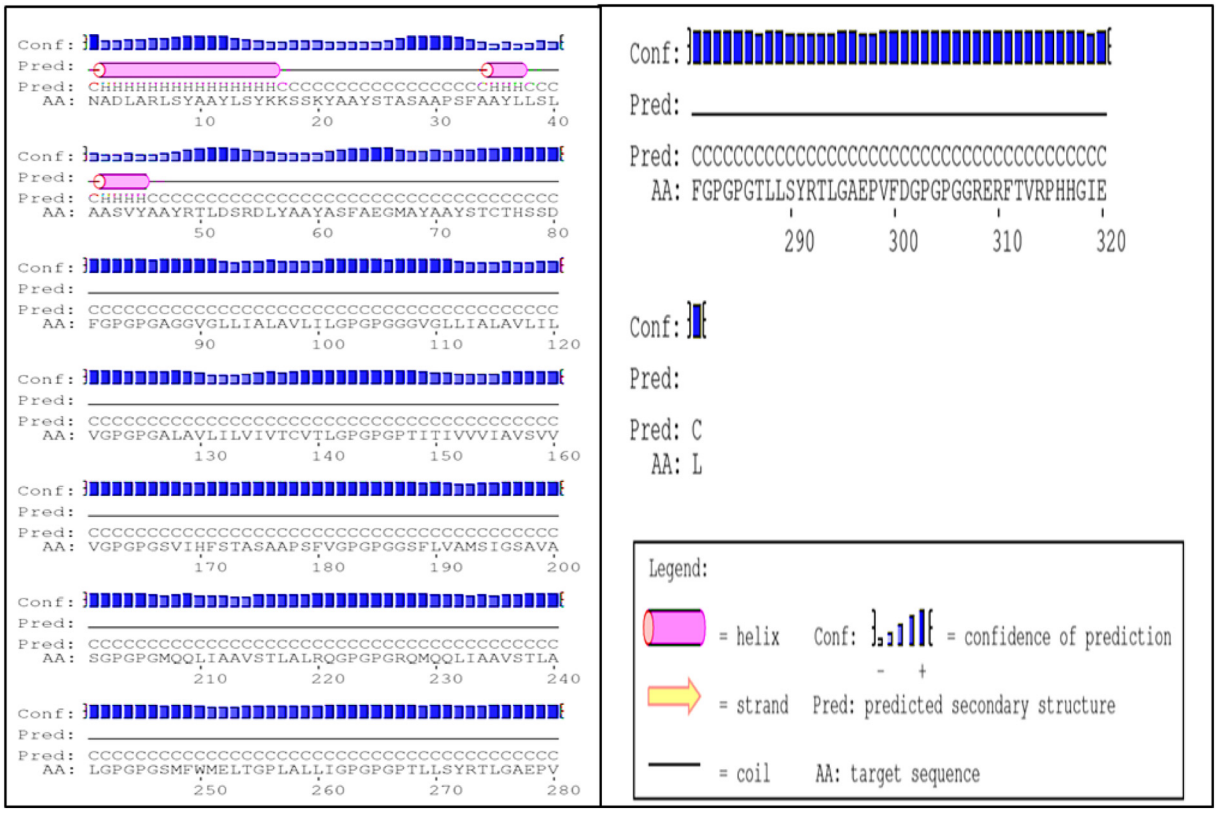

Fig. 4. Graphical depiction of the secondary structure procured for the multi-epitope subunit vaccine construct showing Alpha helix (Hh): 28.04%, Extended strand (Ee): 29.91%, Beta-turn (Tt): 2.18% and Random coil (Cc): 39.88%.

3.12. Tertiary structure validation

The distribution of the Ramachandran map was shown after homology modelling processes in order to validate the 3D vaccine protein models. The Ramachandran plot analysis of refined protein model disclosed that 92.2% of residues lie in the most favourable areas, 4.4% in allowed areas and only 3.4% in disallowed areas (Fig. 5(B)). ERRAT and ProSA-web verified the quality and potential errors in a crude 3D model. A modeled protein's overall quality factor was 76.04% using ERRAT. Although ProSA-web showed a *Z*-score of −4.06, Fig. 5(C), for the given 3D model of vaccine protein model, which lies outside the range of scores commonly found in comparable size native Proteins.

3.13. Molecular docking of subunit vaccine with immune receptor

The targeted docking of protein vaccine against TLR3 was carried out by the PatchDock server. This produced 100 models, which were scored as per the geometry and electrostatic interdependence of the protein surface. FireDock (Fast Interaction Refinement in Molecular Docking) server was used to refine and re-score molecular docking solutions. The refined complexes were ordered according to their binding energy. Among FireDock's top 10 models, based on the assigned binding score for molecular docking, the final complex shown in Fig. 6 was selected for further analysis. The scoring consists of atomic contact energy (1.23), interactions between Van Der Waals (−13.00), partial electrostatics (6.12), and additional binding free energy estimates (−11.97). Moreover, to extract the graphic image of the interaction between the docked complexes, the online database PDBsum and PDBePISA were employed. It created a graphical representation of interactions of the hydrogen bond between the complex of the docked proteins. It was noted that 11 interactions with hydrogen bonds [Chain A (Vaccine)-B (TLR-3); 33–57, 54–56, 175–12, 175–12, 299–198, 325–84, 380–138, 460–29, 462–29, 484–39, and 484–30] with TLR3 and 51 non-bonded interactions were developed in our vaccine construction (Table S3). Structural analysis also revealed that Ser79 and Asp280 formed a hydrogen bond at a distance of 3.21 Å, while Arg227-Asn659 formed a bond at 2.47 Å. Thr268-Thr638 forms a hydrogen bond at a distance of 3.08 Å. Similarly, Pro267-Glu639-639 develops hydrogen bonds at a distance of 3.31 Å and 3.50 Å, Glu278-Asp36 at 3.52 Å, Gly307-200Lys at 2.65 Å, Thr150-Arg331 at 3.41 Å, and Gly266-Ser614 at 2.40 Å, whereas Thr150-Arg331 develop hydrogen bonds at distances of 3.41 Å respectively.

3.14. Root mean square deviation and fluctuation

The ca e complex of final vaccine construct with TLR-3 was subjected to molecular dynamics simulation for stability and residual fluctuation test. RMSD and RMSF of these complexes were calculated and presented in Fig. 7 while RMSD and RMSF graphs for the final vaccine construct only are given in supplementary materials (Fig. S2). In order to assess the stability of final vaccine construct, RMSD of the protein and RMSF of all side chain residues were examined for the time period of 50 ns to find whether the systems show stability or not. The average fluctuation for the system (RMSD) was found to be 2 Å (TLR-3). Residual fluctuation (RMSF) was found to be in acceptable range except for a few, which are in the loop region of the vaccine construct, which showed higher fluctuation.

3.15. Codon optimization of final vaccine constructs

Java Codon Adaptation Tool was employed for optimization of codons to be used in *E. coli* (strain K12), for ensuring the maximum expression of the protein (Fig. 8). Optimized codons sequence length was 963 nucleotides. The Codon Adaptation Index (CAI) of the optimized nucleotide sequence was 0.95, and the average GC content of our

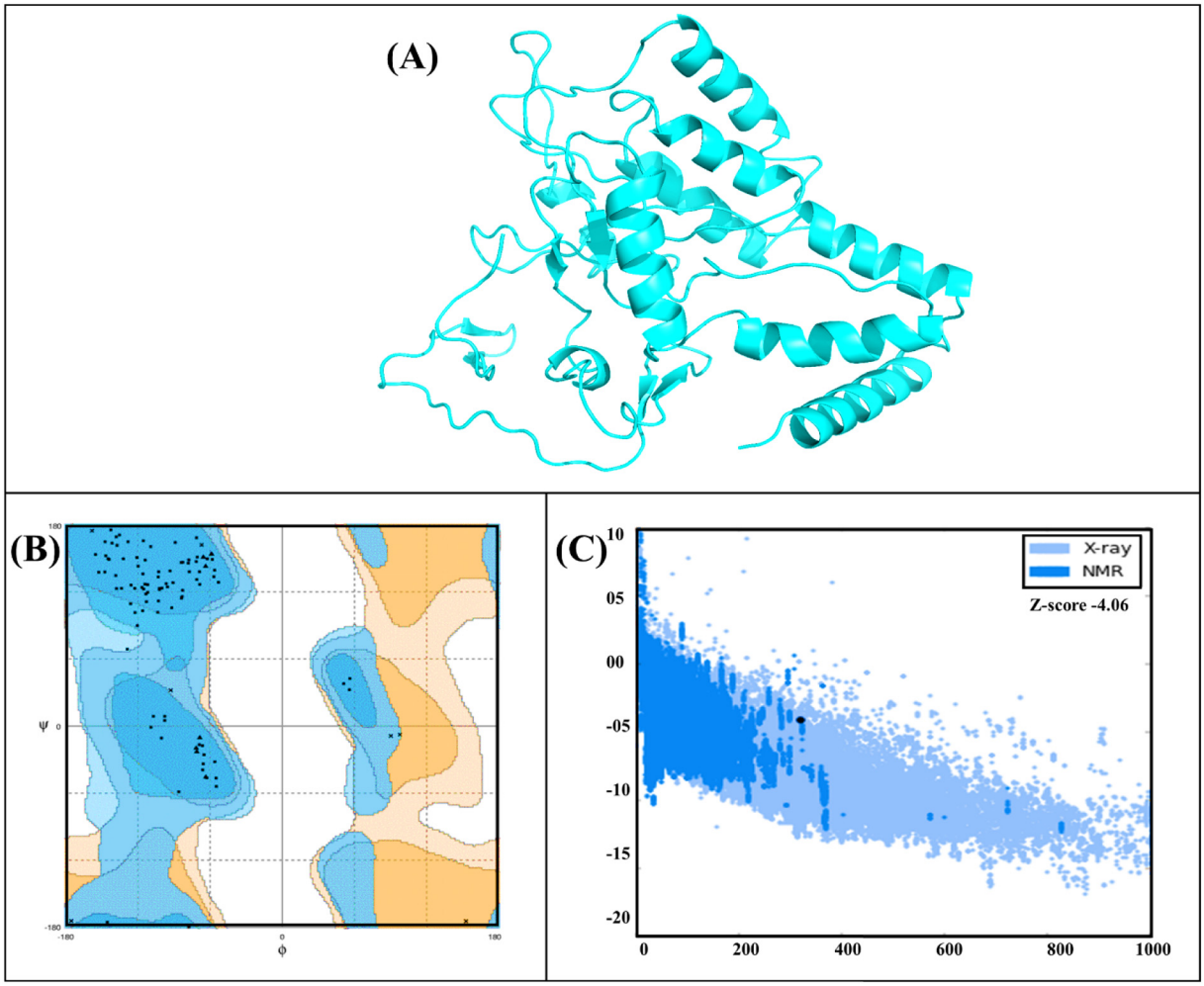

Fig. 5. Structure and validation of the final subunit vaccine model. (a) Here the figure shows the final 3D structure of the multi-epitope subunit vaccine provided after homology modelling and refinement. (b) PROSA 3D structure validation illustrating Z-score (−4.06) and (c) Ramachandran analysis refined model structure showing 92.2%, 4.4% and 3.4%of residues in most favoured, allowed and disallowed regions respectively.

sequence was 58%, which showed that the vaccine protein in *E. coli* could be expressed well. The optimum range of GC content should be between 30% and 70%. The restriction clone was finally formed by inserting the adapted sequences of codons in the pET28a (+) vector.

4. Discussion

The structural polyproteins were selected based on their role in mediating entry of the virus into the host cells and later on in packaging. The structural proteins were found to be inducers of host immune response. Immunization is among the most effective and safe method to control infectious diseases and improve public health efficiently, quickly and cost-effectively. The reliance on specific immunogenic components of pathogens is the main focus of subunit vaccines as compared to the whole pathogen vaccines. Recently the technological advancement and availability of huge genomic and proteomic data expedite the development of subunit vaccine, which probably depends to find potential antigenic targets by applying recent immunoinformatics approaches.

In this study, the identification of MAYV structural polyprotein, prediction of antigenic epitopes, their complex interactions with host MHC alleles and lymphocytes have been investigated for the development of MAYV vaccines. The structural polyproteins were subjected to the BLASTp algorithm of NCBI to check the epitopes sequence similarity with the human proteome. The result indicates that structural polyproteins of MAYV showed no similarity to human host proteins. This strengthens the argument that the MAYV structural polyproteins are ideal antigenic targets for research to develop the subunit vaccine against MAYV infection. Also, B and T cell epitopes were extracted from the previously identified structural proteins. T cells readily identify the peptide epitopes of both the MHC molecules (class I and II), due to its antigenic nature and acknowledged by the T cell receptors (TCR). MHC class I molecules are present in all nucleated cells that represent endogenous proteins or antigens being scanned by the cytosolic pathway and represent the processed antigen to cytotoxic T lymphocytes. MHC class II molecules contain exogenous antigens or pathogen's surface proteins, processed through endocytic pathways to assist the T lymphocytes or CD4 + T cells. The immunoinformatics analysis indicates that our final vaccine protein includes a large number of high-affinity MHC Class I, MHC Class II as well as B-cell linear epitopes based primarily on physiochemical properties and structural characteristics.

The antigenic and non-allergenic score of the final multi-epitope subunit vaccine protein is 0.80 and 1.20 (default threshold set at −0.4) respectively. These values indicate that the final vaccine is antigenic and non-allergenic in nature, which makes it a potent vaccine. The molecular weight of the vaccine protein was 31.7 kDa, which is an average molecular weight for the construction of a multi-epitope subunit vaccine, theoretical PI was 8.54, which implies that the vaccine protein is very basic in nature, the aliphatic index reveals that the protein is occupied by aliphatic side chains, and the instability index

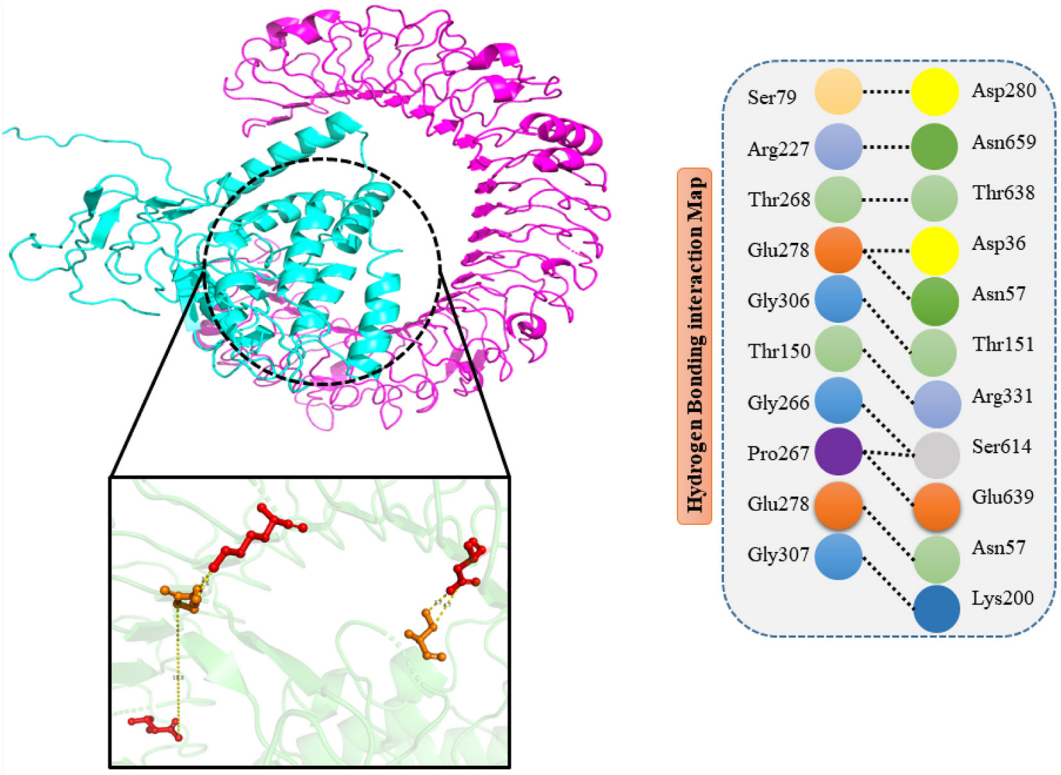

Fig. 6. TLR-3 (PDB ID: 1ZIW)-vaccine docked complex. (A) The TLR-3(receptor) is shown in magenta, while the cyan colour represents the multi-epitope subunit vaccine. The interactions are shown in the side panel. (For interpretation of the references to colour in this figure legend, the reader is referred to the web version of this article.)

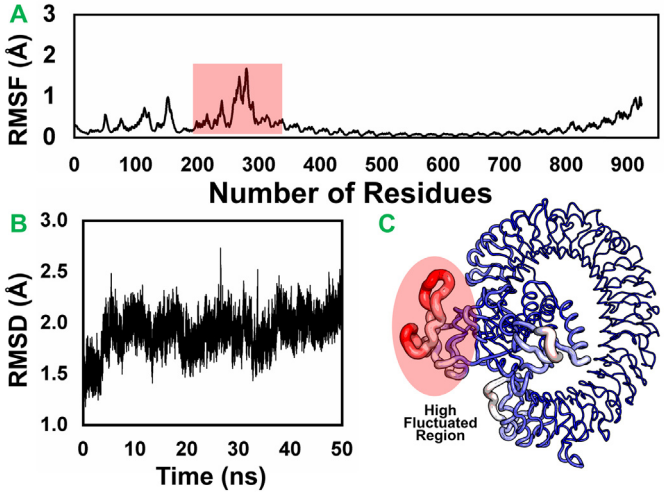

Fig. 7. Molecular dynamics simulation study of protein-vaccine complex representing. (A) Root Mean Square Deviation of the docked complex backbone for the time duration of 50 ns. (B) Root Mean Square Fluctuation representation of the docked complex side chains for the same time duration.

values indicate that the vaccine protein is thermally stable. The secondary vaccine structure predicted by PSIPRED V3.3, showing Alpha helix (Hh): 28.04%, Extended strand (Ee): 29.91%, Beta-turn (Tt): 2.18% and Random coil (Cc): 39.88%.In addition, the 3D structure of the protein was generated by homology modelling with adequate information on the spatial arrangement of essential protein residues, protein normal function, dynamics, interaction with ligand as well as other proteins. Structural validation tools were used to detect errors in the final vaccine structure model structure. We, therefore, conducted docking analysis to comprehend the immune system response of TLR-3 to the vaccine structures. Energy minimization was conducted to minimize the potential energy of the entire system for the overall conformational stability of the docked vaccine protein-TLR-3. Energy minimization repairs the structure's topology by removing steric clashes and thus forms a more relatively stable structure with adequate stereochemistry. The vaccine - TLR-3 complex's predicted RMSD was 2 Å, showing the complex's stability.

For High-level expression of recombinant protein in *E. coli* (strain K12), codon optimization was performed to improve the efficiency of transcription and translation. This was accomplished through the assessment of the DNA sequence's codon adaptation index (CAI) and total GC content. The over-expressed recombinant protein solubility in *E. coli* host is an essential requirement of many biochemical and functional studies. Our protein vaccine in an overexpressed state reveals a permissible proportion of solubility. Improving protein strength is an imperative goal in various biomedical and mechanical applications. Initially designed and tested vaccines in the experimental animal model showed an excellent immunogenic response, but none of them showed the same response when tested in humans due to the complex nature of human immunopathology. We have therefore assimilated completely new immunoinformatics techniques in this study to design a potential, safe and immunogenic subunit vaccine capable of controlling MAYV infection.

5. Conclusion

In this work, with the application of immunoinformatics approaches, we have tried to create a multi-epitope-based subunit vaccine. This scientific study begins with the retrieval of five Mayaro Virus proteins (capsid, E3, E2, 6K and E1) preceded by immunogenic B-cell and T-cell epitope prediction for immunity generation. Predicted epitopes were combined by using appropriate linkers and adjuvant to enhance the immunogenicity of effective epitopes. In this study,

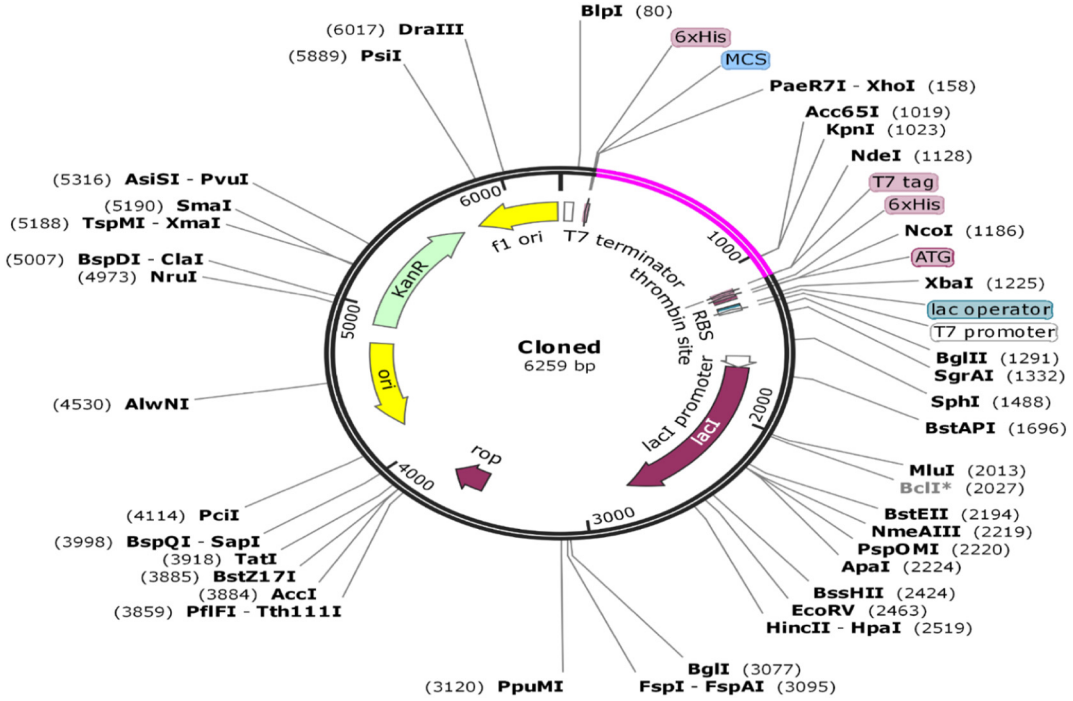

Fig. 8. In silico restriction cloning of the final vaccine construct into pET28a (+) expression vector where purple part representing the vaccine insert and black circle showing the vector. (For interpretation of the references to colour in this figure legend, the reader is referred to the web version of this article.)

allergenicity, antigenicity, physiochemical properties to check the binding affinity and stability of TLR-3 and vaccine complex, molecular docking and dynamics were performed. Finally, disulfide engineering and in silico cloning were carried out to ensure the vaccine construct's stability and effective expression. This research uses a combination of analyses to generate a subunit vaccine construct based on multi-epitope, the proposed vaccine needs to be validated experimentally to ensure the experimental activity. This study will aid infection control by creating an effective immunological memory against *Mayaro's* virus infections.

Conflict of interests

The authors declare no conflict of interest.

Funding and acknowledgment

Dong-Qing Wei is supported by the grants from the Key Research Area Grant 2016YFA0501703 of the Ministry of Science and Technology of China, the National Natural Science Foundation of China (Contract nos. 61832019, 61503244), the Natural Science Foundation of Henan Province (162300410060) and Joint Research Funds for Medical and Engineering and Scientific Research at Shanghai Jiao Tong University (YG2017ZD14). The computations were partially performed at the Center for High-Performance Computing, Shanghai Jiao Tong University.

Authors' contribution

SK, AK, SS, SK, AR, SG and IK conceptualized the methodology. AK, AAK, HK, SS and SK did the analysis. AK, IK and DQW wrote the manuscript. DQW supervised the study. All the authors approved the manuscript.

Appendix A. Supplementary data

Supplementary data to this article can be found online at https://doi.org/10.1016/j.meegid.2019.06.006.

References

Abaitua, F., Rodríguez, J.R., Garzón, A., Rodríguez, D., Esteban, M., 2006. Improving recombinant MVA immune responses: potentiation of the immune responses to HIV-1 with MVA and DNA vectors expressing Env and the cytokines IL-12 and IFN-gamma. Virus Res. 116, 11–20.

Ali, A., Khan, A., Kaushik, A.C., Wang, Y., Ali, S.S., Junaid, M., Saleem, S., Cho, W.C., Mao, X., Wei, D.-Q., 2019. Immunoinformatic and systems biology approaches to predict and validate peptide vaccines against Epstein–Barr virus (EBV). Sci. Rep. 9, 720.

Anderson, C.R., Downs, W.G., Wattley, G.H., Ahin, N.W., Reese, A.A., 1957. Mayaro virus: a new human disease agent. Am. J. Trop. Med. Hyg. 6, 1012–1016.

Andrusier, N., Nussinov, R., Wolfson, H.J., 2007. FireDock: fast interaction refinement in molecular docking. Proteins: Struct., Funct., Bioinf. 69 (1), 139–159.

Benson, D.A., Karsch-Mizrachi, I., Lipman, D.J., Ostell, J., Wheeler, D.L., 2008. GenBank. Nucleic Acids Res. 36, D25.

Coimbra, T.L.M., Santos, C.L., Suzuki, A., Petrella, S., Bisordi, I., Nagamori, A.H., Marti, A.T., Santos, R.N., Fialho, D.M., Lavigne, S., 2007. Mayaro virus: imported cases of human infection in São Paulo state, Brazil. Rev. Inst. Med. Trop. Sao Paulo 49, 221–224.

Colovos, C., Yeates, T.O., 1993. Verification of protein structures: patterns of nonbonded atomic interactions. Protein Sci. 2, 1511–1519.

da Rosa, T., Vasconcelos, P.F., Pinheiro, F., Travassos da Rosa, E.S., Dias, L.B., Cruz, A.C., 1998. Arboviruses isolated in the Evandro Chagas Institute, including some described for the firs time in the Brazilian Amazon Region, their known host, and their pathology for man. In: An Overview of Arbovirology in Brazil and Neighbouring Countries, pp. 20–32.

Dhanda, S.K., Vir, P., Raghava, G.P., 2013. Designing of interferon-gamma inducing MHC class-II binders. Biol. Direct 8, 30.

EL-Manzalawy, Y., Dobbs, D., Honavar, V., 2008. Predicting linear B-cell epitopes using string kernels. J. Mol. Recognit. 21, 243–255 An Interdisciplinary Journal.

Figueiredo, L.T.M., 2007. Emergent arboviruses in Brazil. Rev. Soc. Bras. Med. Trop. 40, 224–229.

Gasteiger, E., Hoogland, C., Gattiker, A., Wilkins, M.R., Appel, R.D., Bairoch, A., 2005. Protein identification and analysis tools on the ExPASy server. In: The Proteomics Protocols Handbook. Springer, pp. 571–607.

Green, D.S., Nunes, A.T., Annunziata, C.M., Zoon, K.C., 2016. Monocyte and interferon based therapy for the treatment of ovarian cancer. Cytokine Growth Factor Rev. 29, 109–115.

Gupta, S., Kapoor, P., Chaudhary, K., Gautam, A., Kumar, R., Raghava, G.P., Consortium, O.S.D.D., 2013. In silico approach for predicting toxicity of peptides and proteins. PLoS One 8, e73957.

Hiramatsu, N., Oze, T., Takehara, T., 2015. Suppression of hepatocellular carcinoma development in hepatitis C patients given interferon-based antiviral therapy. Hepatol. Res. 45, 152–161.

James, C.M., Abdad, M.Y., Mansfield, J.P., Jacobsen, H.K., Vind, A.R., Stumbles, P.A., Bartlett, E.J., 2007. Differential activities of alpha/beta IFN subtypes against influenza virus in vivo and enhancement of specific immune responses in DNA vaccinated mice expressing haemagglutinin and nucleoprotein. Vaccine 25, 1856–1867.
Jiang, W., Ren, L., Jin, N., 2007. HIV-1 DNA vaccine efficacy is enhanced by coadministration with plasmid encoding IFN-α. J. Virol. Methods 146, 266–273.
Källberg, M., Wang, H., Wang, S., Peng, J., Wang, Z., Lu, H., Xu, J., 2012. Template-based protein structure modeling using the RaptorX web server. Nat. Protoc. 7, 1511.
Khan, A., Junaid, M., Kaushik, A.C., Ali, A., Ali, S.S., Mehmood, A., Wei, D.-Q., 2018. Computational identification, characterization and validation of potential antigenic peptide vaccines from hrHPVs E6 proteins using immunoinformatics and computational systems biology approaches. PLoS One 13, e0196484.
Khatoon, N., Pandey, R.K., Prajapati, V.K., 2017. Exploring Leishmania secretory proteins to design B and T cell multi-epitope subunit vaccine using immunoinformatics approach. Sci. Rep. 7, 8285.
Ko, J., Park, H., Heo, L., Seok, C., 2012. GalaxyWEB server for protein structure prediction and refinement. Nucleic Acids Res. 40, W294–W297.
Kühl, U., Lassner, D., von Schlippenbach, J., Poller, W., Schultheiss, H.-P., 2012. Interferon-Beta improves survival in enterovirus-associated cardiomyopathy. J. Am. Coll. Cardiol. 60, 1295–1296.
Larsen, M.V., Lundegaard, C., Lamberth, K., Buus, S., Lund, O., Nielsen, M., 2007. Large-scale validation of methods for cytotoxic T-lymphocyte epitope prediction. BMC Bioinformatics 8, 424.
Lavergne, A., de Thoisy, B., Lacoste, V., Pascalis, H., Pouliquen, J.-F., Mercier, V., Tolou, H., Dussart, P., Morvan, J., Talarmin, A., 2006. Mayaro virus: complete nucleotide sequence and phylogenetic relationships with other alphaviruses. Virus Res. 117, 283–290.
Lee, S.J., Shin, S.J., Lee, M.H., Lee, M.-G., Kang, T.H., Park, W.S., Soh, B.Y., Park, J.H., Shin, Y.K., Kim, H.W., 2014. A potential protein adjuvant derived from *Mycobacterium tuberculosis* Rv0652 enhances dendritic cells-based tumor immunotherapy. PLoS One 9, e104351.
Lin, Z., Zhang, J., Ma, X., Yang, S., Tian, N., Lin, X., Zhou, S., Liu, L., Gao, Y., 2016. The role of interferon lambda 3 genetic polymorphisms in response to interferon therapy in chronic hepatitis B patients: an updated meta-analysis. Hepat. Mon. 16.
Long, K.C., Ziegler, S.A., Thangamani, S., Hausser, N.L., Kochel, T.J., Higgs, S., Tesh, R.B., 2011. Experimental transmission of Mayaro virus by *Aedes aegypti*. Am. J. Trop. Med. Hyg. 85, 750–757.
McGuffin, L.J., Bryson, K., Jones, D.T., 2000. The PSIPRED protein structure prediction server. Bioinformatics 16, 404–405.
Mourão, M.P.G., Bastos, M.d.S., de Figueiredo, R.P., Gimaque, J.B.L., dos Santos Galusso, E., Kramer, V.M., de Oliveira, C.M.C., Naveca, F.G., Figueiredo, L.T.M., 2012. Mayaro fever in the city of Manaus, Brazil, 2007–2008. Vector Borne Zoonotic Dis. 12, 42–46.
Öhlschläger, P., Quetting, M., Alvarez, G., Dürst, M., Gissmann, L., Kaufmann, A.M., 2009. Enhancement of immunogenicity of a therapeutic cervical cancer DNA-based vaccine by co-application of sequence-optimized genetic adjuvants. Int. J. Cancer 125, 189–198.
Pearlman, D.A., Case, D.A., Caldwell, J.W., Ross, W.S., Cheatham III, T.E., DeBolt, S., Ferguson, D., Seibel, G., Kollman, P., 1995. AMBER, a package of computer programs for applying molecular mechanics, normal mode analysis, molecular dynamics and free energy calculations to simulate the structural and energetic properties of molecules. Comput. Phys. Commun. 91, 1–41.
Pinheiro, F.P., Freitas, R.B., da Rosa, J.F.T., Gabbay, Y.B., Mello, W.A., LeDuc, J.W., 1981. An outbreak of Mayaro virus disease in Belterra, Brazil. Am. J. Trop. Med. Hyg. 30, 674–681.
Ponomarenko, J., Bui, H.-H., Li, W., Fusseder, N., Bourne, P.E., Sette, A., Peters, B., 2008. ElliPro: a new structure-based tool for the prediction of antibody epitopes. BMC Bioinformatics 9, 514.
Powers, A.M., Aguilar, P.V., Chandler, L.J., Brault, A.C., Meakins, T.A., Watts, D., Russell, K.L., Olson, J., Vasconcelos, P.F., Da Rosa, A.T., 2006. Genetic relationships among Mayaro and Una viruses suggest distinct patterns of transmission. Am. J. Trop. Med. Hyg. 75, 461–469.
Roe, D.R., Cheatham III, T.E., 2013. PTRAJ and CPPTRAJ: software for processing and analysis of molecular dynamics trajectory data. J. Chem. Theory Comput. 9, 3084–3095.
Rosa, A.P.D.A.T., Pinheiro Filho, F.D.P., Rosa, E.S.T.D., Rodrigues, S.G., Rosa, J.F.S.T.D., Vasconcelos, P.F.D.C., 2000. Arboviroses.
Sabourin, M., Tuzon, C.T., Fisher, T.S., Zakian, V.A., 2007. A flexible protein linker improves the function of epitope-tagged proteins in *Saccharomyces cerevisiae*. Yeast 24, 39–45.
Saha, S., Raghava, G., 2006. AlgPred: prediction of allergenic proteins and mapping of IgE epitopes. Nucleic Acids Res. 34, W202–W209.
Salomon-Ferrer, R., Case, D.A., Walker, R.C., 2013. An overview of the Amber biomolecular simulation package. Wiley Interdiscip. Rev. 3, 198–210.
Schneidman-Duhovny, D., Inbar, Y., Nussinov, R., Wolfson, H.J., 2005. PatchDock and SymmDock: servers for rigid and symmetric docking. Nucleic Acids Res. 33, W363–W367.
Sousa, I.P., Carvalho, C.A., Ferreira, D.F., Weissmüller, G., Rocha, G.M., Silva, J.L., Gomes, A.M., 2011. Envelope lipid-packing as a critical factor for the biological activity and stability of alphavirus particles isolated from mammalian and mosquito cells. J. Biol. Chem. 286, 1730–1736.
Suhrbier, A., Jaffar-Bandjee, M.-C., Gasque, P., 2012. Arthritogenic alphaviruses—an overview. Nat. Rev. Rheumatol. 8, 420.
Toporovski, R., Morrow, M.P., Weiner, D.B., 2010. Interferons as potential adjuvants in prophylactic vaccines. Expert. Opin. Biol. Ther. 10, 1489–1500.
Vasconcelos, P.F., Travassos da Rosa, A., Pinheiro, F.P., Shope, R.E., Travassos da Rosa, J., Rodrigues, S., Dégallier, N., Travassos da Rosa, E., 1998. Arboviruses Pathogenic for Man in Brazil.
Vita, R., Overton, J.A., Greenbaum, J.A., Ponomarenko, J., Clark, J.D., Cantrell, J.R., Wheeler, D.K., Gabbard, J.L., Hix, D., Sette, A., 2014. The immune epitope database (IEDB) 3.0. Nucleic Acids Res. 43, D405–D412.
Wiederstein, M., Sippl, M.J., 2007. ProSA-web: interactive web service for the recognition of errors in three-dimensional structures of proteins. Nucleic Acids Res. 35, W407–W410.